NECROTIZING ENTEROCOLITIS

Necrotizing enterocolitis induces T lymphocyte–mediated injury in the developing mammalian brain

Qinjie Zhou[1,2], Diego F. Niño[1,2], Yukihiro Yamaguchi[1,2], Sanxia Wang[1,2], William B. Fulton[1,2], Hongpeng Jia[1,2], Peng Lu[1,2], Thomas Prindle Jr.[1,2], David Pamies[3,4], Meaghan Morris[5], Liam L. Chen[4], Chhinder P. Sodhi[1,2]*, David J. Hackam[1,2]*

Necrotizing enterocolitis (NEC) causes acute intestinal necrosis in premature infants and is associated with severe neurological impairment. In NEC, Toll-like receptor 4 is activated in the intestinal epithelium, and NEC-associated brain injury is characterized by microglial activation and white matter loss through mechanisms that remain unclear. We now show that the brains of mice and humans with NEC contained $CD4^+$ T lymphocytes that were required for the development of brain injury. Inhibition of T lymphocyte influx into the brains of neonatal mice with NEC reduced inflammation and prevented myelin loss. Adoptive intracerebroventricular delivery of gut T lymphocytes from mice with NEC into *Rag1*$^{-/-}$ recipient mice lacking $CD4^+$ T cells resulted in brain injury. Brain organoids derived from mice with or without NEC and from human neuronal progenitor cells revealed that IFN-γ release by $CD4^+$ T lymphocytes induced microglial activation and myelin loss in the organoids. IFN-γ knockdown in $CD4^+$ T cells derived from mice with NEC abrogated the induction of NEC-associated brain injury after adoptive transfer to naïve *Rag1*$^{-/-}$ recipient mice. T cell receptor sequencing revealed that NEC mouse brain-derived T lymphocytes shared homology with gut T lymphocytes from NEC mice. Intraperitoneal injection of NEC gut-derived $CD4^+$ T lymphocytes into naïve *Rag1*$^{-/-}$ recipient mice induced brain injury, suggesting that gut-derived T lymphocytes could mediate neuroinflammation in NEC. These findings indicate that NEC-associated brain injury may be induced by gut-derived IFN-γ–releasing $CD4^+$ T cells, suggesting that early management of intestinal inflammation in children with NEC could improve neurological outcomes.

INTRODUCTION

Necrotizing enterocolitis (NEC) is the leading cause of death from gastrointestinal disease in premature infants and is characterized by sudden necrosis of the intestine and death in over a third of patients (*1*, *2*). We (*3*, *4*) and others (*5*–*7*) have shown that the development of NEC requires the activation of the lipopolysaccharide receptor Toll-like receptor 4 (TLR4) on the intestinal epithelium, leading to intestinal epithelial cell death and bacterial translocation across the gut into the circulation (*8*, *9*). One of the biggest long-term complications in patients who survive NEC is the development of severe brain injury, which is characterized by loss of myelin and cognitive impairment and is more severe than the brain injury that occurs in premature infants who do not develop NEC (*10*–*12*). We recently showed that NEC-associated brain injury is dependent upon microglial activation in the developing brain, leading to a loss of oligodendrocyte progenitor cells and loss of myelin, findings that were confirmed in human tissue (*13*). The means of communication between the inflamed ileum and the chemical mediators of injury in the newborn brain remain incompletely understood.

To define the potential mechanisms by which inflammation in the gut could lead to injury in the brain, we hypothesized that $CD4^+$ T lymphocytes could play a critical role in the development of NEC-associated brain injury. Here, we show that $CD4^+$ T lymphocytes infiltrated the brains of neonatal mice with NEC and were present in postmortem brain tissue from human infants with NEC. These $CD4^+$ T lymphocytes were required for NEC-associated brain injury in the neonatal mice, as inhibition of lymphocyte influx into the brain led to neuroprotection. Using brain organoid cultures derived from mouse and human induced pluripotent stem cells (iPSCs), we further showed that lymphocytes exerted their neuroinflammatory effects through the release of interferon-γ (IFN-γ). Inhibition of IFN-γ release or blocking $CD4^+$ T lymphocyte activity prevented NEC-associated brain injury, whereas direct intracerebroventricular injection of NEC-associated gut lymphocytes caused brain injury in naïve *Rag1*$^{-/-}$ recipient mice. T cell receptor sequencing of the lymphocytes in the brains of neonatal mice with NEC revealed marked homology with gut-derived lymphocyte clones from neonatal mice with NEC, suggesting a gut origin of the brain-infiltrating T cells.

RESULTS

NEC in mice and humans leads to microglial activation and an influx of $CD4^+$ T lymphocytes into the injured brain

To interrogate a possible immunological basis for the development of NEC-associated brain injury, we first sought to define the presence and identity of lymphocytes in the newborn brain in mice and humans with and without NEC. Examination of the brains of human infants with NEC compared with control infants who had died from an unrelated condition of prematurity revealed an increased accumulation of $CD4^+$ T lymphocytes (Fig. 1, A and B). The brains of infants with NEC also showed increased expression of the microglia activation marker ionized calcium binding adaptor molecule 1 (Iba1), consistent with the presence of activated microglia in the human NEC brain (Fig. 1C).

[1]Division of General Pediatric Surgery, Johns Hopkins University and Bloomberg Children's Center, Johns Hopkins Hospital, Baltimore, MD, USA. [2]Department of Surgery, Johns Hopkins University School of Medicine, Baltimore, MD, USA. [3]Center for Alternatives to Animal Testing, Johns Hopkins School of Public Health, Baltimore, MD, USA. [4]Department of Biomedical Science, University of Lausanne, Lausanne, Switzerland. [5]Division of Neuropathology, Department of Pathology, Johns Hopkins School of Medicine, Baltimore, MD, USA.
*Corresponding author. Email: dhackam1@jhmi.edu (D.J.H.); csodhi@jhmi.edu (C.P.S.)

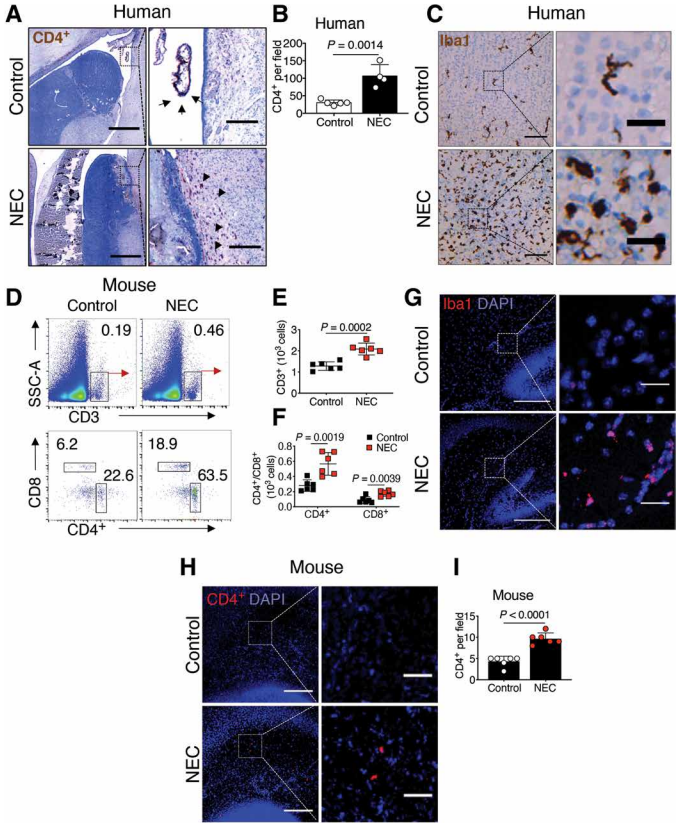

Fig. 1. Brains of newborn human infants and mice with NEC show accumulation of CD4$^+$ T lymphocytes. (**A**) Representative photomicrographs of 3,3′-diaminobenzidine immunostaining for CD4$^+$ T cells in brain sections from autopsy specimens of 36-week-old infants with NEC and age-matched control infants without NEC. Scale bars, 1 mm (left) and 200 μm (right). Black arrowheads indicate infiltration of CD4$^+$ T cells into the brain parenchyma (bottom). (**B**) Quantification of immunohistochemical staining for CD4$^+$ T cells in the periventricular area of the brains of NEC and control infants. Quantification was performed based on immunohistochemical staining of brain sections from four NEC and five control cases. (**C**) Representative photomicrographs of 3,3′-diaminobenzidine immunostaining for the microglial activation marker Iba1 in the periventricular brain region of premature human infants with NEC or control infants without NEC. Scale bars, 200 μm (left) and 5 μm (right). (**D**) Representative flow cytometry plot showing the numbers of CD3$^+$, CD3$^+$CD4$^+$, and CD3$^+$CD8$^+$ T cells in control and NEC mouse brains. (**E** and **F**) Quantification of CD3$^+$ and CD3$^+$CD4$^+$ T cells in perfused mouse brains from NEC and age-matched control mice ($n = 6$ for each group). (**G**) Representative photomicrographs for immunohistochemical staining for Iba1 in the hippocampal area of sagittal brain sections from control and NEC mice. Scale bars, 200 μm (left) and 25 μm (right). DAPI, 4′,6-diamidino-2-phenylindole. (**H**) Representative photomicrographs and (**I**) quantification of tomato-red CD4$^+$ T cells in the hippocampal area in perfused brains from NEC and age-matched control mice ($n = 6$ for each group). Scale bars, 100 μm (left) and 25 μm (right). Cleared mouse brain slices were scanned under a confocal microscope by z stack of 60 steps with 5-μm depth for each step and subjected to maximum intensity projection using FIJI software. Experiments were performed in triplicate with at least six mice per group per experiment. Statistical differences were determined using unpaired two-tailed Student's *t* test.

Similar findings were also seen in the brains of mice with experimentally induced NEC (Fig. 1, D and E). In this mouse model, NEC was induced in neonatal mice through a combination of gavage of milk-based formula, twice daily exposure to hypoxia, and oral administration of bacteria from the stool of an infant with severe NEC. Flow cytometric analysis of perfused mouse brain tissue revealed a significant increase in CD3$^+$ T lymphocytes in the brains of mice with NEC compared to age-matched control mice ($P = 0.0002$; Fig. 1, D and E); on further analysis, this increase was found to be due to CD4$^+$ and CD8$^+$ T cells ($P = 0.0019$; Fig. 1F). Confocal microscopy further revealed increased expression of the microglial activation marker Iba1 in the brains of mice with NEC compared to age-matched control mice (Fig. 1G). This correlated with a significant increase in the accumulation of CD4$^+$ T cells as revealed by immunostaining in the brains of mice with NEC compared to age-matched control mice ($P < 0.0001$; Fig. 1, H and I).

In the gut of NEC mice, we observed inflammation and histological evidence of damage to the ileum, which mimicked that seen in the human NEC gut (fig. S1, A to C). Mice with NEC developed marked brain injury manifested by a loss of myelin basic protein in the midbrain ($P = 0.0042$; fig. S1, D and E) and by microglial activation (Fig. 1G). Brain injury in NEC mice was also indicated by the expression of the proinflammatory cytokine *Tnfα* ($P = 0.0068$; fig. S1F) and the neuroinflammatory marker lipocalin-2 (*Lcn2*) ($P = 0.0005$; fig. S1G), both of which have been validated as markers of injury in the premature brain (*14*). The accumulation of CD4$^+$ T cells in the brains of mice with NEC was observed within the hippocampus, corpus callosum, and midbrain (Fig. 1, H and I; fig. S2, D and E). Activated microglia in the brains of mice with NEC were distributed in the hippocampus, frontal cortex, and midbrain, with little increase in the cerebellum (fig. S2, A to C); there was also little CD4$^+$ T cell accumulation in the cerebellum (fig. S2, D and E).

To further assess microglial activation in NEC-associated brain injury, we next assessed the relative degree to which the microglia exhibited either a ramified (nonactivated) or ameboid (activated) morphology, a known morphological indicator of microglial activation (*15*). To do so, we experimentally induced NEC, this time in *Cx3cr1*-GFP mice that expressed green fluorescent protein (GFP) driven by the microglial cell promoter *Cx3cr1* (*16*). We then performed unbiased morphometric analysis of GFP staining in mouse brain slices. As shown in fig. S3 (A and B), there was a significant increase in ameboid-shaped GFP-expressing cells in the hippocampus in mice with NEC compared to control mice ($P = 0.0174$), which was consistent with the microglial activation observed in Fig. 1. Furthermore, there was a significantly greater effect of brain injury at later stages of development, specifically at postnatal day 10 (P10) compared to P7, as manifested by increased expression of *Lcn2* and decreased expression of *Mbp* when comparing the brains of mice with and without NEC ($P < 0.05$; fig. S3, C and D). Mice with more severe intestinal manifestations of NEC, including higher expression of the injury marker *Lcn2* in the intestine, also had more severe brain injury indicated by higher expression of *Lcn2* in the brain (fig. S3E). Last, to gain insights into how CD4$^+$ T lymphocytes might accumulate in the brain, we assessed the blood-brain barrier in mice with NEC using the fluorescein dextran permeabilization assay (*17*). We identified a relative loss of blood-brain barrier integrity in NEC mice compared to control mice (fig. S3F). In control experiments, renal endothelial barrier integrity was determined to be intact in mice with NEC (fig. S3F), suggesting specificity of the inflammatory response for the brain.

Accumulation of CD4$^+$ T lymphocytes in the newborn mouse brain is required for development of NEC-associated brain injury

We determined the nature of the lymphocytes present in the brains of mice with NEC using flow cytometric analysis. The CD4$^+$ T cells

in NEC mouse brains were predominantly T helper 17 (T_H17) (Rorγt$^+$) and T_H1 (T-bet$^+$) populations, both of which were significantly elevated in mice with NEC compared to control mice (T-bet$^+$, $P = 0.0022$; Rorγt$^+$, $P < 0.0001$; fig. S4, A to C). T_H2 (Gata3$^+$) and T_{reg} (Foxp3$^+$) populations were similar between NEC and control mouse brains (fig. S4, A, D, and E). The CD4$^+$ T lymphocytes that accumulated in the brains of mice with NEC showed significantly increased IFN-γ staining ($P = 0.0006$) but similar interleukin-17 (IL-17) staining when compared with control mouse brains (fig. S4, F to H).

We next sought to address whether accumulating CD4$^+$ T lymphocytes were a cause or a consequence of brain injury. To do so, we injected the sphingosine-1-phosphate (S1P) receptor inhibitor FTY720, which prevents lymphocyte egress from secondary lymphoid tissues (*18*). Injection of FTY720 prevented the infiltration of CD4$^+$ T cells into the brains of mice with NEC as revealed by flow cytometry (fig. S5, A and B). There were three major effects including reduced expression of proinflammatory cytokines *Tnfα* and *Lcn2*, which was indicative of reduced inflammation in the brain (Fig. 2, A and B). There was also reduced microglial activation as evidenced by reduced expression of *Iba1* (Fig. 2, E and G, and fig. S5I), which we have shown to be required for the initiation of NEC-associated brain injury. In addition, the preservation of myelination in the brain was consistent with reduced brain injury (Fig. 2, F and H, and fig. S5J). The T cell inhibition strategy did not limit the development of NEC injury in the intestine, as revealed by persistently elevated proinflammatory cytokine expression and histology in the ileum (fig. S5, C to E). Thus, the cerebroprotective effects of T cell inhibition could not be explained by a simple abrogation of NEC severity.

Next, to confirm that the rescue phenotype was due to inhibition of CD4$^+$ T cells and not other potential S1P1-expressing cells, we injected wild-type mice one day after the induction of NEC with a monoclonal CD4$^+$ T cell neutralizing antibody (fig. S5A) (*19*). This reduced CD4$^+$ T cell infiltration into the mouse brain (fig. S5B), the expression of proinflammatory cytokines (Fig. 2, C and D), and microglial activation (Fig. 2, E and G, and fig. S5I) and restored myelin basic protein expression (Fig. 2, F and H, and fig. S5J), without ameliorating inflammation in the ileum (fig. S5, F to H).

CD4$^+$ T lymphocytes from NEC mouse brains induce brain injury in recipient mice

To investigate further the role of brain parenchymal CD4$^+$ T lymphocytes in the development of NEC-associated brain injury, we next harvested CD4$^+$ T lymphocytes from the brains of mice with NEC (NEC brain-T cells) or without NEC (control brain-T cells) and injected these cells into the lateral ventricles of non-NEC naïve *Rag1*$^{-/-}$ recipient mice, which lack T cells and B cells (Fig. 3A). The efficiency of the adoptive transfer was assessed after tissue clearing

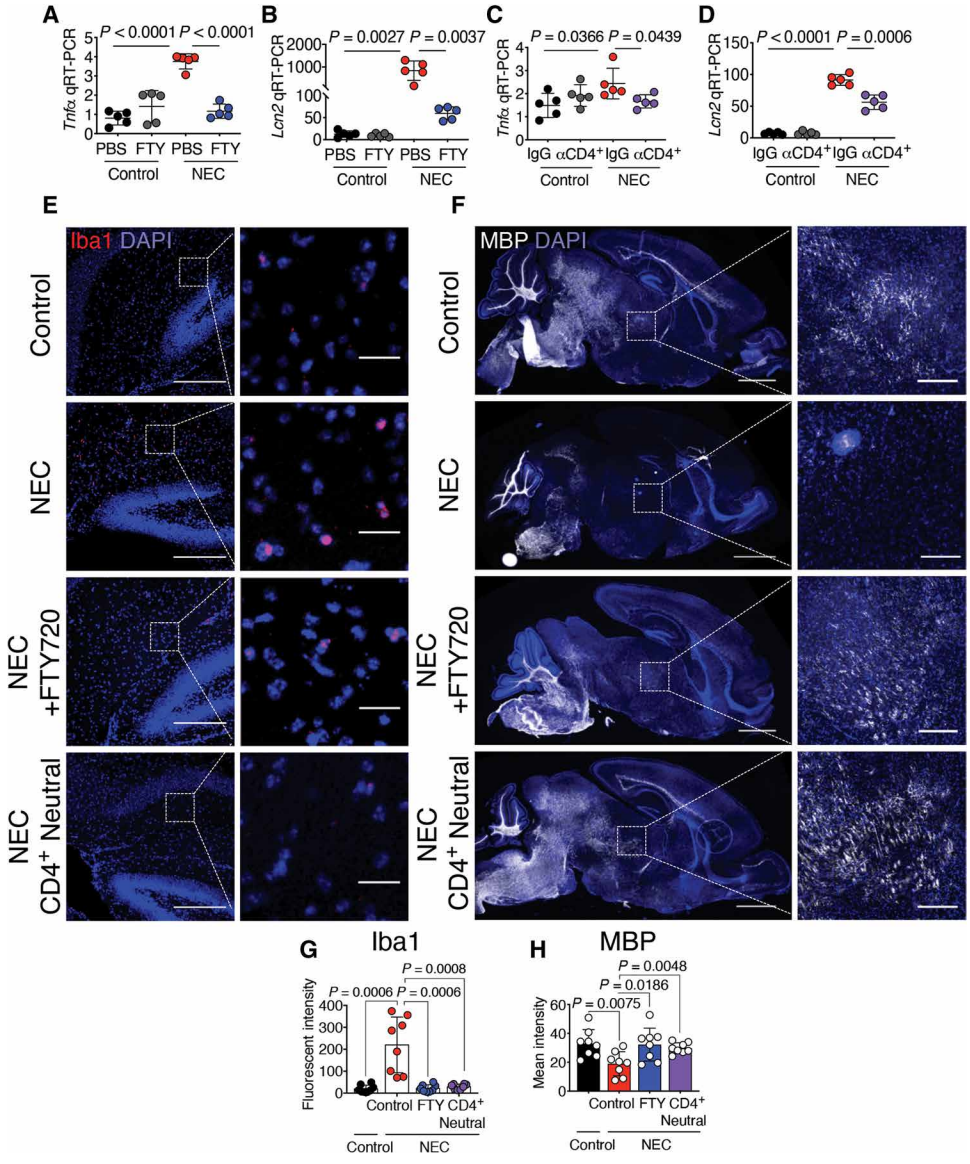

Fig. 2. NEC-associated brain injury requires CD4$^+$ T lymphocyte accumulation in newborn mouse brain. (**A** to **D**) Quantitative real-time PCR (qRT-PCR) analysis of *Tnfα* and *Lipocalin-2* (*Lcn2*) expression in the brains of control or NEC mice treated with vehicle, FTY720 (FTY) (which inhibits lymphocyte egress from lymphoid tissues), or CD4$^+$ T cell neutralizing antibody ($n = 5$ for each group, repeated twice). (**E** and **F**) Representative photomicrographs showing immunohistochemical staining for the microglial activation marker Iba1 (E) and myelin basic protein (MBP) (F) in the hippocampal area (E) or sagittal whole-brain sections (F) of control or NEC mice treated with vehicle, FTY720, or CD4$^+$ T cell neutralizing antibody (CD4$^+$ Neutral). Scale bars, (E) 200 μm (Iba1, left) and 25 μm (Iba1, right); (F) 1 mm (MBP, left) and 150 μm (MBP, right). (**G** and **H**) Quantification of Iba1 and MBP immunostaining in brain sections represented in (E) and (F). Experiments were repeated three times with at least three animals per group in each experiment. Statistical significance was analyzed using unpaired two tailed Student's *t* test.

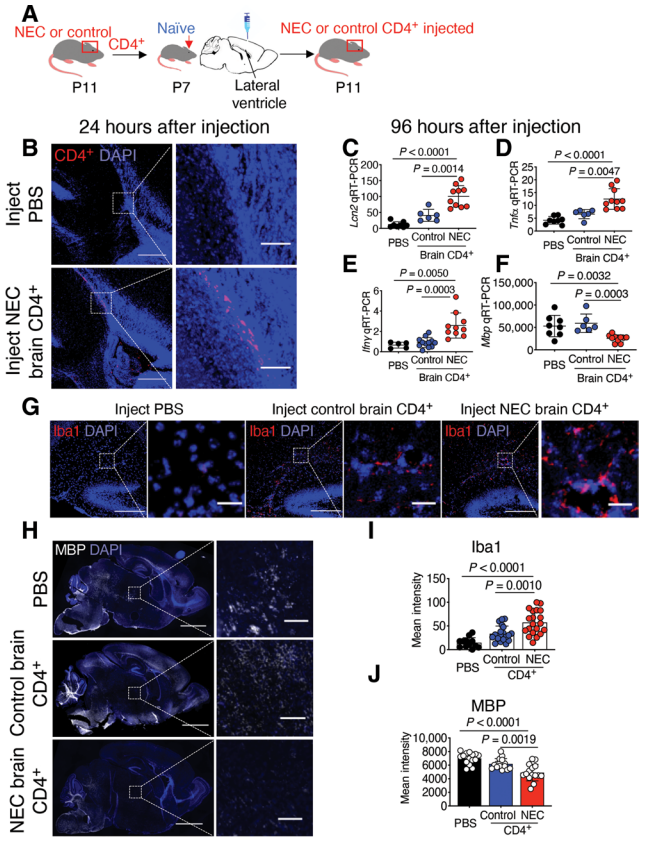

Fig. 3. CD4$^+$ T lymphocyte accumulation in the NEC mouse brain induces NEC-associated brain injury. (**A**) Schematic showing adoptive transfer of brain-infiltrating CD4$^+$ T cells from NEC or control mouse brains into naïve *Rag1*$^{-/-}$ recipient mice by intracerebroventricular injection. (**B**) Representative photomicrographs of the lateral ventricular area in cleared brain tissue from naïve *Rag1*$^{-/-}$ recipient mice 24 hours after intracerebroventricular injection of NEC or control mouse brain-infiltrating tomato-red CD4$^+$ T cells or PBS as a control. Scale bars, 200 μm (left) and 25 μm (right). (**C** to **F**) qRT-PCR analysis of expression of (C) *Lcn2* ($n = 5$), (D) *Tnfα* ($n \geq 6$), (E) *Ifnγ* ($n \geq 5$), and (F) *Mbp* ($n \geq 6$) in mouse forebrains 96 hours after intracerebroventricular injection with NEC or control brain-infiltrating CD4$^+$ T cells or PBS as a control. (**G** and **H**) Representative photomicrographs showing immunohistochemical staining for Iba1 or MBP in the hippocampal area or sagittal whole-brain sections of *Rag1*$^{-/-}$ recipient mice 96 hours after intracerebroventricular injection of NEC or control mouse brain-infiltrating tomato-red CD4$^+$ T cells or PBS as a control. Scale bars, 200 μm (Iba1, left), 25 μm (Iba1, right), 1 mm (MBP, left), and 150 μm (MBP, right). (**I** and **J**) Quantification of Iba1 ($n \geq 12$) or MBP ($n \geq 15$) in immunohistochemically stained hippocampal or whole-brain sections from these groups. Brain samples from three to five animals were analyzed from three independent experiments. Image analysis and quantification were performed within the indicated region of interest (ROI) obtained from midsagittal whole-brain sections using FIJI software. Statistical significance was determined by two-tailed Student's *t* test.

of mouse brain sections (*20*), which revealed CD4$^+$ T cells within the lateral ventricles and the corpus callosum 24 hours after injection (Fig. 3B and movie S1). Compared with mouse brains that were injected with either phosphate-buffered saline (PBS) or control brain-T cells, the injection of NEC brain-T cells induced a marked increase in the expression of *Tnfα*, *Lcn2*, and *Ifnγ* in the mouse forebrain (Fig. 3, C to E), revealing inflammation in the brain at 96 hours after injection. There was also increased expression of Iba1 in the hippocampal and corpus callosum areas (Figs. 3, G and I), consistent with microglial activation. The injection of NEC brain-T cells also induced a significant loss of myelin quantified in the midbrain ($P = 0.0019$; Fig. 3, F, H, and J), as indicated by immunostaining for myelin basic protein and quantitative real-time polymerase chain reaction (qRT-PCR). There was no microglial activation or loss of myelin basic protein in mouse brains after the injection of either PBS or control brain-T cells (Fig. 3, C to J). These findings illustrate that CD4$^+$ T cells in the brains of mice with NEC could be sufficient to cause the induction of proinflammatory cytokines, activation of microglia, and the loss of myelin.

NEC brain-derived T cells indirectly induce inflammation in a mouse brain organoid model system

We next sought to determine whether the CD4$^+$ T lymphocytes that accumulate in the brains of mice with NEC cause a loss of myelin through cell-dependent or cell-independent mechanisms. To distinguish between these two possibilities, we established a three-dimensional mouse brain organoid system in culture in which mouse brain organoids were grown on top of a permeable Transwell filter insert (Fig. 4A). NEC brain-derived CD4$^+$ T lymphocytes were added either directly to the mouse brain organoids (to test for direct effects) or to the chamber under the Transwell insert such that any molecules released from the CD4$^+$ T lymphocytes would only exert effects indirectly. Figure 4 shows the pattern of expression in the brain organoids of genes linked to the development of immature neurons [Nestin (*Nes*)], mature neurons [neurofilament heavy polypeptide (*Nefh*)], oligodendrocyte precursor cells [oligodendrocyte transcription factor 2 (*Olig2*) and neuron-glial antigen 2 (*Ng2*)], mature oligodendrocytes (*Mbp*), microglia (*Iba1*), and astrocytes [glial fibrillary acidic protein (*Gfap*)] (Fig. 4, B to E, and fig. S6, A to C). The gene expression data indicated that each of these cell types existed in the cultured mouse brain organoids (Fig. 4, B to E, and fig. S6, A to C). The extent of myelination increased as the organoids were maintained in culture over a 4-week period (Fig. 4F). The addition of CD4$^+$ T cells from the brains of control mice to the cultured mouse brain organoids for 7 days had no effect on either cytokine induction (Fig. 4, G and H) or myelination (Fig. 4, I and J). By contrast, the direct addition of NEC brain-T cells to the cultured mouse brain organoids for 7 days resulted in a marked induction of *Tnfα* and *Lcn2* expression (Fig. 4, G and H) and a significant loss of myelin as revealed by myelin basic protein immunostaining ($P = 0.0001$; Fig. 4, I and J). To evaluate whether this effect was attributable to the release of secreted molecules, we repeated this experiment by placing the NEC brain-T cells into a separate compartment isolated from the cultured mouse brain organoids by a 0.4-μm Transwell polyester membrane. This experimental setup still resulted in a significant increase in cytokine expression in the cultured mouse brain organoids (*Tnfα*, $P = 0.0011$; *Lcn2*, $P = 0.0292$; Fig. 4, K and L) and a reduction in the degree of myelination of the neurons (Fig. 4, M and N).

IFN-γ release mediates the effects of NEC brain-derived T cells on mouse brain organoids

To define the potential mechanisms by which NEC brain-T cells could induce inflammation and injury when injected into mouse brains, we next focused on our observation that these NEC brain-derived CD4$^+$ T cells could be induced to release IFN-γ, and we sought to investigate whether IFN-γ could play a role in the setting of NEC-associated brain injury. The addition of recombinant IFN-γ to cultured mouse brain organoids for 24 hours increased the

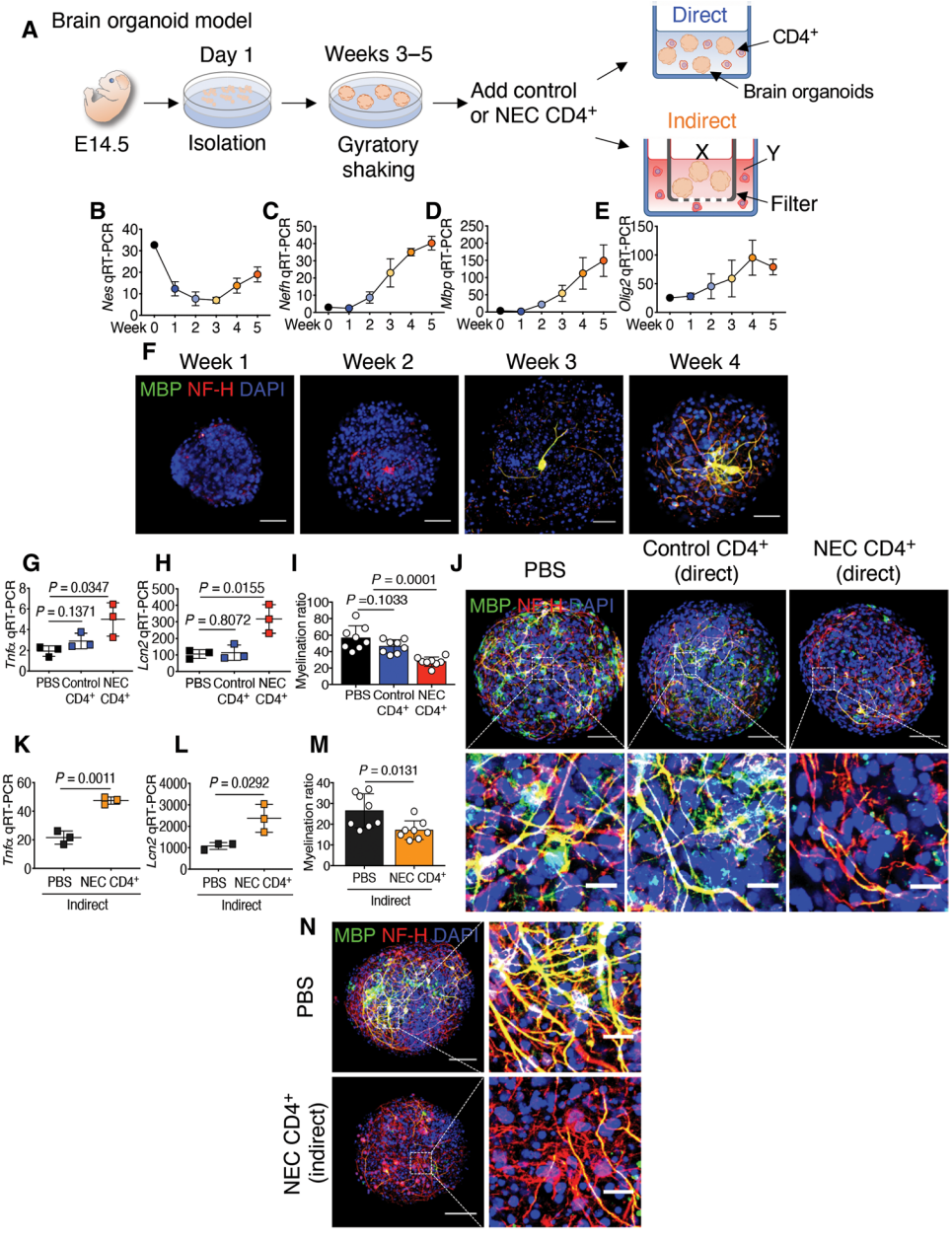

Fig. 4. CD4$^+$ T lymphocytes from NEC mouse brains induce hypomyelination in mouse brain organoid cultures. (**A**) Schematic shows generation of 3D mouse brain organoids in vitro. Mouse brain organoids were treated directly with CD4$^+$ T cells isolated from NEC mouse brains or control mouse brains or indirectly in a Transwell culture system. In the indirect treatment studies, mouse brain organoids were cultured in compartment X and NEC mouse brain CD4$^+$ T cells were added to compartment Y. (**B** to **E**) Weekly qRT-PCR analysis of expression of (B) *Nestin* (*Nes*), (C) neurofilament heavy polypeptide (*Nefh*), (D) *Mbp*, and (E) *Olig2* in mouse brain organoids from week 1 to week 5 of culture ($n = 3$ for each time point from week 1 to week 5). Expression for each gene at week 0, which corresponds to the time point when brain organoid culture began, is also shown. (**F**) Representative photomicrographs of mouse brain organoids at weeks 1 to 4 of culture, immunostained for MBP (green), neurofilament heavy polypeptide (NF-H, red), and DAPI nuclear stain (blue). Scale bars, 50 μm. (**G** and **H**) qRT-PCR analysis of expression of (G) *Tnfα* and (H) *Lcn2* in mouse brain organoids treated directly with CD4$^+$ T cells isolated from NEC mouse brains or control mouse brains, or PBS. (**K** and **L**) qRT-PCR analysis of expression of (K) *Tnfα* and (L) *Lcn2* in mouse brain organoids treated indirectly with CD4$^+$ T cells isolated from NEC mouse brains or PBS in the Transwell culture system. Mouse brain organoids were treated with 5000 CD4$^+$ T cells/ml starting from week 3 of culture for 1 week and were harvested at week 4 of culture ($n = 3$ samples for each group). (**I** and **M**) Quantification of myelination in mouse brain organoids treated directly (I) or indirectly (M) with CD4$^+$ T cells isolated from NEC mouse brains or control mouse brains, or PBS. (**J** and **N**) Representative photomicrographs showing immunostaining for MBP (green), NF-H (red), and DAPI (blue) in mouse brain organoids treated directly (J) or indirectly (N) with CD4$^+$ T cells isolated from NEC mouse brains or control mouse brains, or PBS ($n = 8$ brain organoids for each group). Scale bars, 50 μm (left) and 5 μm (right). Statistical significance was determined by Student's *t* test.

expression of *Tnfα* and *Lcn2* (Fig. 5, A and B) and induced a loss of myelin (Fig. 5, C to E) in the organoids. To assess whether these findings had potential relevance to human NEC-associated brain injury, we next used brain organoids derived from human inducible pluripotent stem cells (iPSCs) (Fig. 5, F to J). The treatment of human brain organoids in culture with IFN-γ induced an inflammatory response characterized by the induction of *IL-1β* and the neuroinflammatory marker *LCN2*. There was also a reduction in myelination as indicated by decreased expression of the myelin marker myelin-associated glycoprotein (*MAG*) and reduced immunohistochemical staining for myelin basic protein (Fig. 5, F to J). To determine whether IFN-γ release from NEC brain-T cells could explain the loss of myelin and the expression of proinflammatory cytokine genes, we next treated mouse brain-derived organoids with NEC brain-T cells in the presence of either IFN-γ–neutralizing antibody or isotype control antibody. Treatment of mouse brain organoids with IFN-γ–neutralizing antibody, but not the isotype control antibody, significantly reduced the induced expression of *Tnfα* ($P = 0.0357$) and *Lcn2* ($P = 0.0002$) by the NEC brain-T cells (Fig. 5, K to L), indicating a reduction in the inflammatory response. There was also a partial restoration of myelination in the mouse brain organoids, as indicated by myelin basic protein staining (Fig. 5, M and N).

IFN-γ release from CD4$^+$ T cells is required for NEC-associated brain injury in mice

Our findings suggested that the CD4$^+$ T cells that accumulated in the brains of NEC mice could have induced NEC-associated brain injury through the release of IFN-γ. To test this possibility, we first

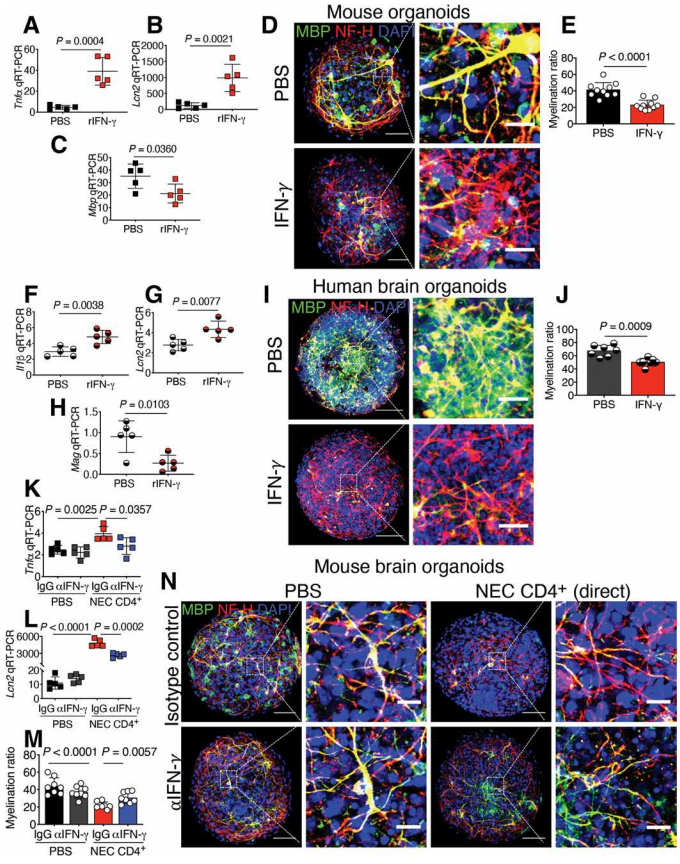

Fig. 5. IFN-γ release mediates the effects of NEC brain-T cells on demyelination in cultured brain organoids. (**A** to **C** and **F** to **H**) qRT-PCR analysis of *Tnfα*, *Lcn2*, and *Mbp* gene expression in mouse (A to C) or human (F to H) brain organoids in culture treated with recombinant IFN-γ ($n = 5$ samples for each group). (**D** and **I**) Representative photomicrographs of immunohistochemical staining for MBP (green) and NF-H (red) and (**E** and **J**) quantification of the myelination ratio in mouse [(D), $n = 10$] or human [(I), $n = 7$] brain organoids in culture treated with recombinant IFN-γ. Specifically, mouse brain organoids (after 3 weeks in culture) or human brain organoids (after 5 weeks in culture) were treated with IFN-γ (200 U/ml for 24 hours), and culture was continued with IFN-γ–free medium before harvest at week 4 (mouse) or week 6 (human) of culture. (**K** and **L**) qRT-PCR analysis of expression of (K) *Tnfα* and (L) *Lcn2* in mouse brain organoids treated directly with $CD4^+$ T cells isolated from NEC mouse brains in the presence of IFN-γ–neutralizing antibody or isotype control IgG ($n = 5$ samples for each group). Specifically, mouse brain organoids (after 3 weeks in culture) were treated with purified NEC brain-derived $CD4^+$ T cells at 5000 cells/ml in the presence of IFN-γ–neutralizing antibody or control IgG at 10 mg/ml. Culture medium was replenished with fresh medium containing IFN-γ–neutralizing antibody or control IgG at 10 mg/ml after 3 days, and mouse organoids were harvested 1 week after initiation of the coculture with $CD4^+$ T cells (a total of 4 weeks in culture). (**M**) Myelination ratio quantification and (**N**) representative photomicrographs of MBP and NF-H immunohistochemical staining of mouse brain organoids treated with purified NEC brain-derived $CD4^+$ T cells in the presence of IFN-γ–neutralizing antibody or control IgG ($n = 8$ brain organoids for each group). Scale bars, 50 μm (left) and 5 μm (right). Statistical significance was determined by Student's *t* test.

measured the concentration of IFN-γ in the brains of mice with NEC compared with age-matched controls and determined that the concentration of IFN-γ in NEC mouse brains was significantly higher compared with control brains ($P = 0.0085$; Fig. 6A). To assess the functional relevance of this observation, recombinant IFN-γ was injected into the lateral ventricles of naïve mouse recipients at the age at which NEC usually emerges. This resulted in significant microglial activation as revealed by increased staining for the Iba1 marker ($P = 0.0002$; Fig. 6, B and C), as well as increased expression of the proinflammatory cytokine genes *Tnfα* and *Lcn2* (Fig. 6, D and E). IFN-γ injection also caused a loss of myelin in the brain both globally and in the midbrain area, linking IFN-γ release to the hypomyelination phenotype observed in NEC mouse brains (Fig. 6, F and G). Next, to evaluate whether IFN-γ release was required for the induction of brain inflammation in NEC mice, we used an *Ifnγ* knockdown strategy in which NEC brain-T cells were treated with *Ifnγ* short hairpin RNAs (shRNAs) for 24 hours ex vivo to knock down IFN-γ. After confirmation of *Ifnγ* knockdown (Fig. 6H), these NEC brain-T cells were then injected directly into the brains of naïve $Rag1^{-/-}$ mice at P7, and the brains were harvested on P11 to assess for brain injury. The injection of NEC brain-T cells treated with scrambled shRNA into $Rag1^{-/-}$ mouse brains still induced brain injury characterized by expression of *Lcn2* (Fig. 6I) and Iba1 (Fig. 6, J and K), as would be expected. By contrast, injection of NEC brain-T cells treated with *Ifnγ* shRNAs to knock down *Ifnγ* into $Rag1^{-/-}$ mouse brains resulted in minimal brain injury, as revealed by low *Lcn2* expression (Fig. 6I) and minimal Iba1 activation (Fig. 6, J and K).

In an additional confirmatory experiment, we directly injected brains of NEC mice with IFN-γ–neutralizing antibody or control isotype immunoglobulin G (IgG) on day 2 after initiation of NEC (fig. S7A). We observed that intracerebral injection of IFN-γ–neutralizing antibody, but not control IgG, significantly reduced the degree of NEC-associated brain injury, as revealed by a reduction in microglial activation ($P = 0.0003$; fig. S7, B and C), reduced expression of *Tfnα* ($P = 0.0065$) and *Lcn2* ($P = 0.0006$) (fig. S7, D and E), and preservation of myelin in the brain ($P = 0.0017$; fig. S7, F and G).

Gut-derived T cells contribute to NEC-associated brain injury

Last, we sought to evaluate the source of the $CD4^+$ T cells that accumulated and caused injury in the brains of mice with NEC. Given our previous work indicating that the development of NEC requires the accumulation of $CD4^+$ T lymphocytes in the intestines of newborn mice and humans (*21*), we considered whether the NEC brain-derived T lymphocytes originated from the inflamed intestines in the setting of NEC. We first obtained $CD4^+$ T lymphocytes from the intestines of mice with NEC and tested their potential effects in both the mouse brain organoid culture system (Fig. 7, A to F) and after direct injection into the mouse brain (Fig. 7, G to L). As shown in Fig. 7 (B and C), the addition of NEC gut-derived $CD4^+$ T cells to cultured mouse brain organoids resulted in increased expression of the proinflammatory molecules *Tnfα* and *Lcn2*. These gut-derived T lymphocytes also induced a significant loss of myelin basic protein and demyelination in the organoids (qRT-PCR, $P = 0.0320$; myelination ratio, $P = 0.0075$; Fig. 7, D to F), suggesting that the lymphocytes originating from the inflamed intestines of NEC mice could induce brain injury. To test this possibility directly in vivo, we harvested $CD4^+$ T lymphocytes from the intestines of mice with NEC and injected them (intracerebroventricularly) into the brains of $Rag1^{-/-}$ mice at P7, which is the age at which NEC is induced in our experimental mouse model. As shown in Fig. 7 (G to L), intracerebral injection of NEC gut-derived $CD4^+$ T lymphocytes resulted in a significant induced expression of *Tnfα* ($P = 0.0213$) and *Lcn2* ($P = 0.0015$) in the mouse brain (Fig. 7, G and H), the activation of microglia (Fig. 7, I and K), and a notable loss of myelin (Fig. 7, J and L).

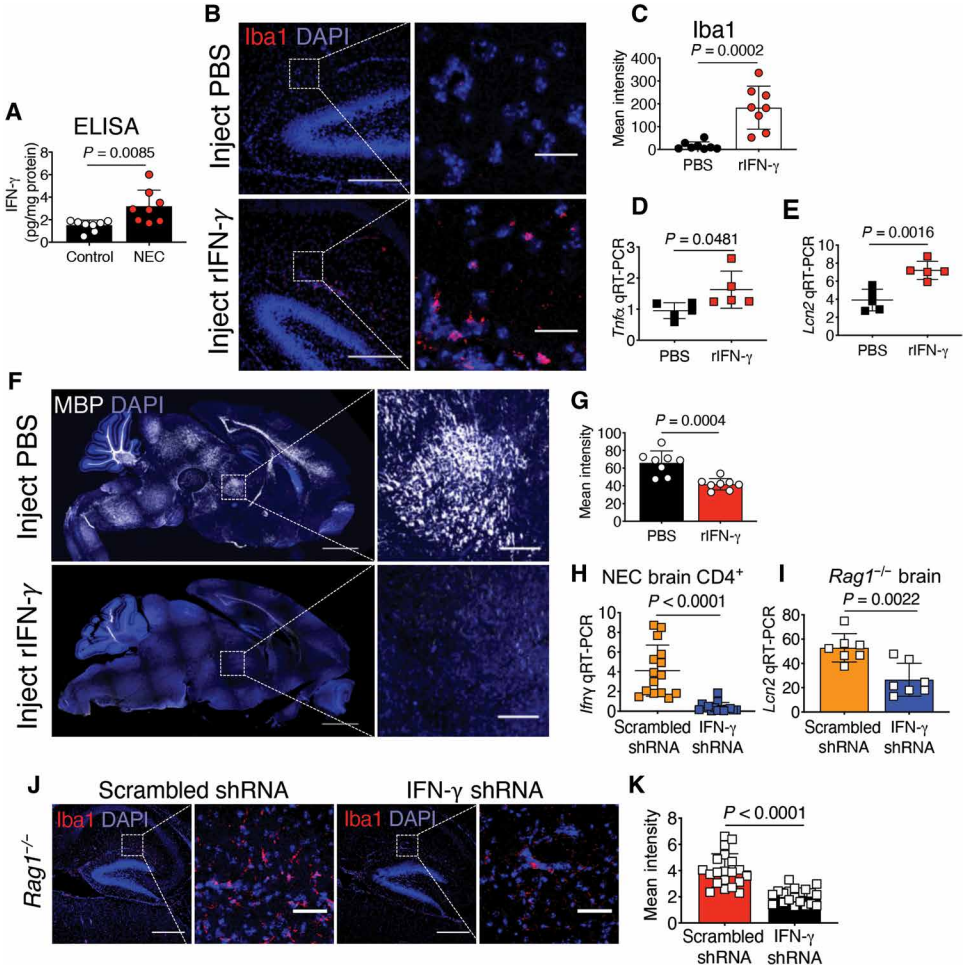

Fig. 6. IFN-γ release from CD4$^+$ T lymphocytes mediates induction of NEC-associated brain injury in mice. (**A**) Enzyme-linked immunosorbent assay (ELISA) analysis of IFN-γ in NEC mouse brains and age-matched control mouse brains 4 days after initiation of NEC in the NEC mouse model ($n = 8$ for each group). (**B** and **F**) Representative photomicrographs and (**C** and **G**) quantification of Iba1 or MBP immunostaining in the hippocampal area or sagittal whole-brain sections from either IFN-γ– or PBS-injected mouse recipients assessed at P11 ($n = 8$ for each group). IFN-γ (10,000 U per recipient) was injected intracerebroventricularly into wild-type control mouse brains at postnatal day 7 (P7), with injury assessment at postnatal day 11 (P11). Scale bars, 200 μm (Iba1, left), 25 μm (Iba1, right), 1 mm (MBP, left), and 150 μm (MBP, right). (**D** and **E**) qRT-PCR analysis of expression of (D) *Tnfα* and (E) *Lcn2* in mouse brains injected intracerebroventricularly with either IFN-γ or PBS ($n = 5$ for each group). (**H**) qRT-PCR analysis of expression of *Ifnγ* in CD4$^+$ T lymphocytes obtained from the brains of NEC mice after lentiviral vector–mediated delivery of *Ifnγ* shRNA or scrambled shRNA. (**I** to **K**) qRT-PCR analysis of expression of *Lcn2* (I) and representative photomicrographs showing Iba1 staining (J) and quantification (K) in *Rag1*$^{-/-}$ mouse brains after intracerebroventricular injection of NEC brain-derived T cells treated with scrambled or *Ifnγ* shRNA ($n \geq 7$ for each group). Three independent experiments were performed with at least three mice per group per experiment. Statistical significance was determined by Student's *t* test.

We next sought to investigate more directly whether CD4$^+$ T lymphocytes could migrate from the gut to the brain of NEC mice. To do so, we obtained CD4$^+$ T lymphocytes from the intestines of 11-day-old wild-type C57BL/6 mice that were either control or induced to develop NEC. These gut-derived CD4$^+$ T cells were injected into the peritoneum of *Rag1*$^{-/-}$ mice and assessed for whether they would cause brain injury. We observed a marked induction of brain injury 18 hours later in the *Rag1*$^{-/-}$ mouse recipients that had received the intraperitoneal injection of CD4$^+$ T cells from NEC mouse intestines, as revealed by increased brain expression of *Lcn2* and Iba1 (Fig. 8, A to C). There was no brain injury seen in *Rag1*$^{-/-}$ mouse recipients that were injected intraperitoneally with PBS or with CD4$^+$ T cells derived from the intestines of breast-fed mice without NEC, excluding a simple neuroinflammatory effect of intraperitoneal injection alone.

Last, to further establish whether the CD4$^+$ T lymphocytes that we detected in the brains of mice with NEC were derived from the mouse intestine, we performed sequencing analysis of the T cell receptors of gut- and brain-derived T lymphocytes, focusing on the signature TCRB V-D-J rearrangements. As shown in Fig. 8D, in five separate T cell samples from mice with NEC, we observed an average 25% overlap (25.21 ± 3.951; $n = 5$) between the clones of T cells from the gut and the brain, compared to an average 2% overlap (1.975 ± 0.205; $n = 5$) observed in the lymphocytes from the gut and brain of control mice (Fig. 8E). Together, these findings suggest that NEC-associated brain injury was mediated by CD4$^+$ T lymphocytes releasing *Ifnγ*, some of which may have been derived from the gut.

DISCUSSION

There is growing evidence that various neurological diseases previously thought to lack an immunological basis are influenced by the activation of the immune system (*22*). Such immunologically mediated neuropathies include multiple sclerosis (*23*), stroke/ischemia-reperfusion injury (*24*, *25*), and the neurological consequences of cerebral malaria (*26*). In the current study, we report that CD4$^+$ T lymphocytes, partially of intestinal origin, damage the developing brain of neonatal mice in the setting of NEC through the release of IFN-γ. The inhibition of CD4$^+$ T lymphocyte influx into the NEC mouse brain yielded protection against NEC-associated brain injury. In contrast, direct intracerebroventricular injection into *Rag1*$^{-/-}$ naïve recipient mouse brains of brain-derived T lymphocytes from mice with NEC resulted in myelin loss and proinflammatory cytokine gene expression. In seeking to define the mechanisms involved, we determined that the injection of the neonatal mouse brain with IFN-γ, or the addition of IFN-γ to cultured mouse brain organoids, mimicked the role of brain-infiltrating T cells, whereas strategies to block IFN-γ release from these T lymphocytes protected NEC mice from brain injury. Together, these findings suggest a mechanism by which brain injury occurs in NEC through the infiltration of T lymphocytes into the brain that release IFN-γ, and

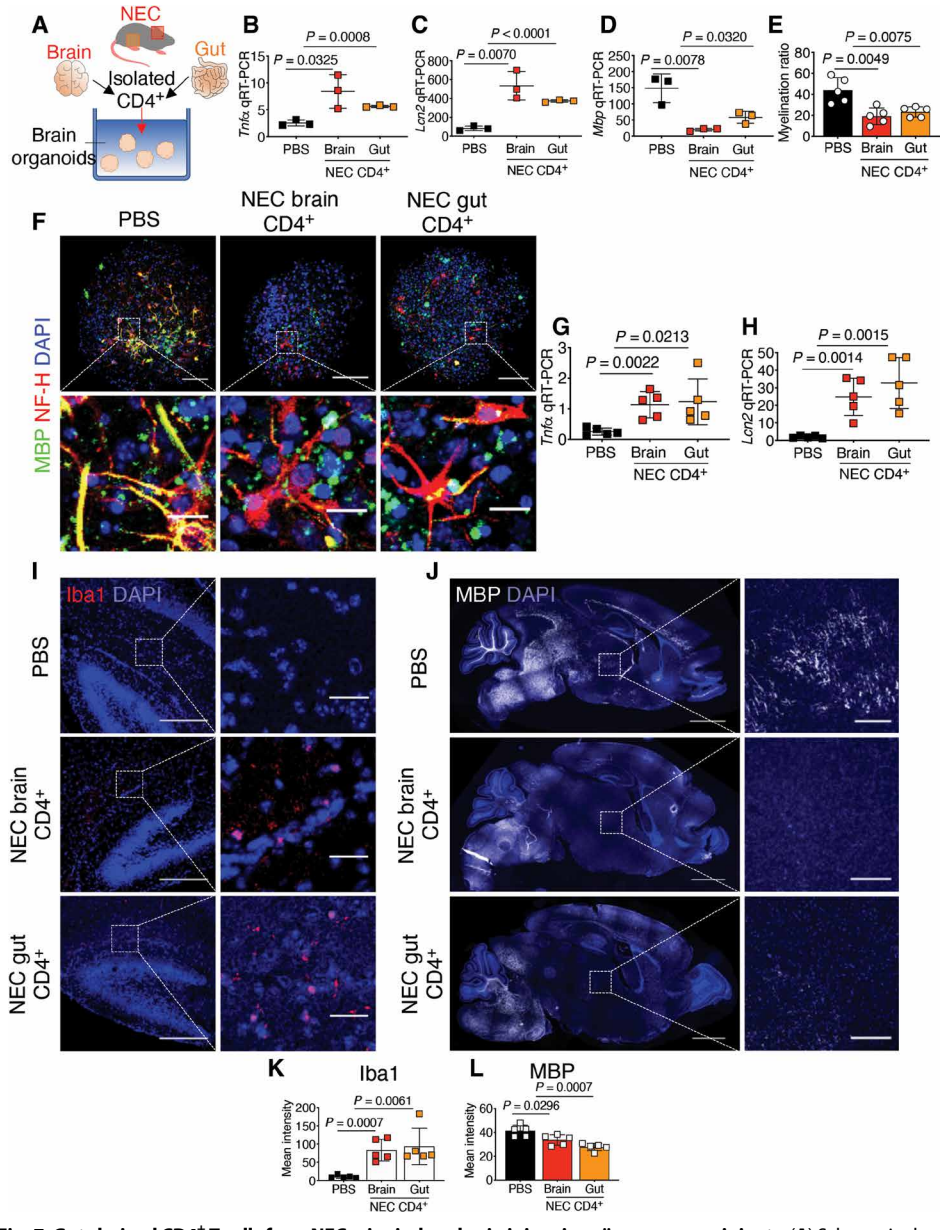

Fig. 7. Gut-derived CD4$^+$ T cells from NEC mice induce brain injury in naïve mouse recipients. (**A**) Schematic shows mouse brain organoids in culture treated with NEC brain-derived CD4$^+$ T cells (5000 cells/ml), NEC gut-derived CD4$^+$ T cells (5000 cells/ml), or PBS as a control starting at week 3 of culture. Mouse brain organoids were harvested for assessment at week 4 of culture. (**B** to **D**) qRT-PCR analysis of expression of *Tnfα* (B), *Lcn2* (C), and *Mbp* (D) in mouse brain organoids in culture treated with NEC brain-derived CD4$^+$ T cells, NEC gut-derived CD4$^+$ T cells, or PBS as a control ($n = 3$ samples for each group). (**E**) Myelination quantification and (**F**) representative photomicrographs of MBP (green) and NF-H (red) immunohistochemical staining of mouse brain organoids treated with NEC brain-derived CD4$^+$ T cells, NEC gut-derived CD4$^+$ T cells, or PBS as a control ($n = 5$ brain organoids for each group). (**G**) qRT-PCR analysis of expression of (G) *Tnfα* and (**H**) *Lcn2* in mouse forebrains after intracerebroventricular injection of NEC brain-derived CD4$^+$ T cells, NEC gut-derived CD4$^+$ T cells, or PBS as a control into naïve recipient mice ($n = 5$ for each group). (**I** and **J**) Representative photomicrographs and (**K** and **L**) quantification of Iba1 and MBP immunohistochemical staining in the hippocampal area or sagittal whole-brain sections of naïve recipient mice after intracerebroventricular injection of NEC brain-derived CD4$^+$ T cells, NEC gut-derived CD4$^+$ T cells, or PBS as a control ($n = 5$ for each group). Scale bars, 200 μm (Iba1, left), 25 μm (Iba1, right), 1 mm (MBP, left), and 150 μm (MBP, right). Statistical significance was determined by two-tailed Student's *t* test.

The role of T cells as primary mediators of NEC-associated brain injury extends our understanding of the myriad roles that activated T cells play in the newborn brain. An influx of T_H17-like lymphocytes was reported to mediate neonatal hypoxic-ischemic brain injury (*27*). Other studies have reported that splenectomy that reduces available CD4$^+$ T cells or *Rag1*$^{-/-}$ neonatal mice that congenitally lack CD4$^+$ T cells protected against hypoxic-ischemic brain injury (*28*, *29*). Our finding that IFN-γ played a critical role in the development of NEC-associated brain injury in our neonatal mouse model is supported by previous work showing an enrichment in IFN-γ in experimental allergic encephalomyelitis, a mouse model of multiple sclerosis (*30*). In this model, a subgroup of T_H17 cells stopped producing IL-17 and secreted IFN-γ instead, resulting in brain injury (*31*). In seeking to understand the mechanisms by which IFN-γ release could lead to brain injury, we note that IFN-γ release is known to cause the activation of microglia (*32*). We report here that microglial activation occurred in the brains of mice with NEC and was necessary for the hypomyelination of neurons that characterized NEC-associated brain injury in our neonatal mouse model. In addition to studying the effects of T lymphocytes in the brains of mice with experimental NEC, we also used a brain organoid culture system where we combined either mouse or human brain organoids with lymphocytes and their effector molecules.

There are several limitations to the current work. First, the precise antigen or group of antigens that was responsible for activating the T cells and recruiting them to the brain in the setting of NEC resulting in IFN-γ release and brain injury remains unknown. It is tempting to speculate based on previous studies that central nervous system antigens such as myelin products could activate T cells, suggesting that such molecules could also serve as potential neuroprotective targets (*33*, *34*). Such antigens could pass through either the permeable blood-brain barrier or the lymphatic system and activate CD4$^+$ T cells in the periphery, resulting in their infiltration into the developing brain. Given that activated T lymphocytes were required for NEC induction, a gut origin for the activated T lymphocytes seemed likely and it is possible that antigens within the intestine provide a rationale for neuroprotective strategies based upon limiting the deleterious effects of immune activation in this vulnerable period of life.

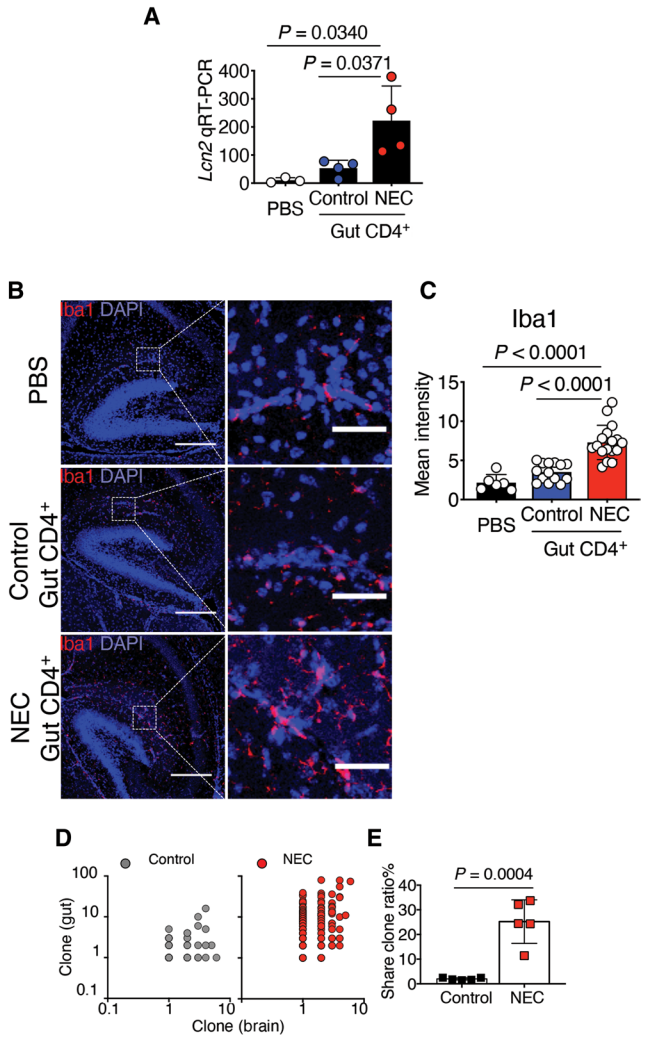

Fig. 8. Brain injury is induced in naïve recipient mice by gut-derived CD4$^+$ T lymphocytes from NEC mice. (**A** to **C**) qRT-PCR expression of *Lcn2* (A) and representative confocal micrographs showing the expression and quantification of Iba1 (B and C) in the brains of *Rag1*$^{-/-}$ recipient mice that had been injected intraperitoneally 18 hours earlier with gut-derived CD4$^+$ T lymphocytes from mice with NEC, control mice without NEC, or PBS. Representative of three separate experiments with at least three mice per group in each experiment. Scale bars, 200 μm (Iba1, left) and 25 μm (Iba1, right). Statistical significance was determined by Student's *t* test (C). (**D** and **E**) Pairwise scatter plots showing shared T cell receptor sequencing clones between control mouse brain and control mouse gut (gray), and NEC mouse brain and NEC mouse gut (red). (E) Shared clone ratio. Five mice were pooled for each data point to reach a sufficient clone number for meaningful analysis, and five data points were submitted for sequencing for each group (control mouse brain, control mouse gut, NEC mouse brain, and NEC mouse gut). Statistical significance was determined by two-tailed Student's *t* test.

could have played a role in T cell activation. NEC is known to largely occur in formula-fed infants, and a link between diet, nutrition, and T cell development has been established (*35*, *36*). It is possible that specific components of infant formula, as well as the effects of diet on the gut microbiota, could lead to the initial priming and activation of CD4$^+$ T cells in the periphery. Alternatively, metabolic stressors induced in the formula-fed infants may result in T cell activation, as is known to occur in the setting of diet-induced metabolic stress (*37*). Furthermore, the direct evidence of T cells trafficking from gut to brain has been demonstrated in an ischemic stroke rodent model where intestinal γδ T cells migrated to the brain (*38*) and in a chronic mouse colitis model where gut-derived CD4$^+$ T cells were shown to traffic into brain meninges and contribute to cerebral inflammation (*39*). Additional limitations of our study include the fact that it did not completely exclude the role of other inflammatory cells, such as neutrophils (*40*), macrophages (*41*), or CD8$^+$ T cells (*42*), that could interact with CD4$^+$ T cells to cause NEC-associated brain injury. Our study was also limited by our dependence on a neonatal mouse model of NEC that was not an exact replicate of the human disease (*43*). Our study adds to an expanding body of work examining the link between NEC and brain injury in mouse (*44*) and also piglet models (*45*, *46*), and there is increasing interest in a potential role of the gut microbiota (*47*). Last, we acknowledge that the human brain control samples were not perfectly age-matched and fully comparable to the NEC human brain samples, although they were all obtained from preterm infants without NEC.

Our new findings of CD4$^+$ T cells contributing to the development of NEC-associated brain injury need to be integrated with our previous work showing a critical role for TLR4 signaling in the pathogenesis of NEC in the gut. Specifically, we have shown that activation of TLR4 in the newborn intestinal epithelium by a dysbiotic gut microbiota leads to destruction of the intestinal barrier, bacterial translocation into the circulation, and the development of NEC with subsequent activation of brain microglia by epithelial release of high mobility group box 1 (HMGB1) (*48*). Release of inflammatory mediators from the gut in response to epithelial TLR4 signaling could lead to the activation of CD4$^+$ T lymphocytes in the intestine, which could then traffic to the brain to cause microglial activation and subsequent brain injury. The finding that HMGB1 leads to T lymphocyte release of IFN-γ (*49*, *50*) integrates our new findings with our earlier work.

We have shown that NEC-associated brain injury required T cell activation and release of IFN-γ, resulting in microglia activation and myelin loss in the NEC mouse brain. These T cells share homology with intestinal lymphocytes, providing insights into their organ of origin, and suggesting that strategies to inhibit T cells could be a potential treatment for NEC-associated brain injury. Current clinical practice dictates that the care of patients with NEC should be directed toward controlling intestinal injury and preventing the development of systemic sepsis. This long-standing therapeutic framework has guided strategies that include cessation of oral feeding, the initiation of broad-spectrum antibiotics, and the use of surgery to remove dead or dying intestinal tissue. However, our study now suggests that this protocol needs to be updated to include considerations of the brain as well as the gut in NEC treatment strategies. A revised approach would include rapid escalation of medical care and the early removal of inflamed intestinal tissue to prevent brain injury and improve neurocognitive outcomes.

MATERIALS AND METHODS

Study design

The overall objective of the study was to test the hypothesis that infiltrating T cells mediate the development of NEC-associated brain injury. This was tested using a neonatal mouse model of NEC and by examination of human brain tissue and cultured mouse and human brain organoids. All experiments and animal protocols were approved by the Johns Hopkins University in accordance

with the *Guide for the Care and Use of Laboratory Animals* (8th edition, The National Academies Press, 2011). For genetically modified mice, all mice were backcrossed at least eight times with C57BL/6 wild-type mice.

A power analysis was performed for each experiment. To detect differences ($P < 0.05$) in each study criterion, three to eight animals per group were required. The precise number of animals per group is shown by dots in each figure and in the figure legends. All data points were included for evaluation; in mouse models of NEC, all points were included, and outliers were included in the statistical analysis and included as raw data points in each of the figures. Mouse pups of the same gestational age were randomized to each group without bias to size. Both genders were used in equal ratios in all experiments. All data examination and histologic assessment were performed on samples that were blinded to the study group. The number of times experiments were repeated varied by experiment and are included in each figure legend. The precise number of samples is included in each figure as a separate dot.

Human brain samples were obtained with approval from the Johns Hopkins University School of Medicine Institutional Review Board (#15-06-17-01RD) in accordance with the Johns Hopkins University anatomical tissue procurement guidelines. Human brain samples were obtained at autopsy from infants who died with a diagnosis of NEC or from control infants who died from non-NEC causes and without any clinical evidence of brain pathology. Gestational age, age at death, and postmortem interval for all cases (NEC $n = 4$ and control $n = 5$) are provided in table S1.

Mouse strains and experiments

Strains C57BL/6, *Rag1*$^{-/-}$ (B6.129S7-Rag1tm1Mom/J, stock 002216), CD4CreERT2 [B6(129X1)-Tg(Cd4-cre/ERT2)11Gnri/J, stock 022356], and CX3CR1-GFP [B6.129P2(Cg)-Cx3cr1tm1Litt/J, stock 005582] were purchased from The Jackson Laboratory (Bar Harbor, ME). CD4$^+$-Tomato reporter mice (CD4$^+$-tomato-red) were generated by breeding B6.Cg-Gt(ROSA)26Sortm9(CAG-tdTomato) Hze/J stock 007909 mice with CD4-CreER-T2 [B6(129X1)-Tg(Cd4-cre/ERT2)11Gnri/J] mice. Tamoxifen was orally administered (0.4 μg per mouse per day for 2 days), 48 hours before the onset of experimentation. For intracerebroventricular injection, 7-day-old (for injected lymphocytes) or 8-day-old (for injected antibodies) mouse pups were cryo-anesthetized by placing on ice for 1 to 2 min, and then placed in a stereotaxic device (Stoelting, Wood Dale, IL, USA). Purified lymphocytes (harvested as described below) or reagents (antibody or inhibitor) were suspended in ice-cold PBS, loaded into a 10-μl Hamilton syringe injector (model 1701 RN, needle at 26s gauge, 2 inch, point style 2, 80030, Hamilton, Nevada, USA), and injected perpendicularly to the skull surface at 2 mm deep into both lateral ventricles by applying gentle pressure to the plunger over the course of 30 to 60 s with a maximum volume of 2 μl for each side. The injection needle was removed 15 s after discontinuation of the injection to prevent backflow. After the injection procedure, mice were placed into a warm environment to regain normal body temperature and respiratory function before returning to their cages. In all cases, 5 to 10 mice were injected for each group. Mortality rate was below 10%, and tissue harvest occurred at P11. For lymphocyte injection experiments, 10,000 cells in total were injected into the brains of each pup. For IFN-γ–related studies, 10,000 U of recombinant IFN-γ or 30 μg of IFN-γ–neutralizing antibody in total was injected per animal.

Induction of experimental NEC

NEC was induced in 7-day-old mouse pups (P7), which were gavage-fed with formula (Similac Advance Infant Formula, Abbott Nutrition) and Esbilac canine milk replacer (PetAg) at a ratio of 2:1, supplemented with enteric bacteria isolated from an infant with NEC five times daily for 4 days. In addition, mice were exposed to brief hypoxia (5% O_2, 95% N_2) for 10 min twice daily during the 4-day model. Breast-fed control animals were kept with the dam until the time of euthanasia. This experimental protocol induces patchy necrosis of the ileum and up-regulation of inflammatory cytokines in the intestinal mucosa, which resemble the pathologic findings of human NEC. Small intestine was harvested on day 11 and subjected to hematoxylin and eosin staining on 5-μm-thick paraffin-embedded cross sections with imaging performed on a Leica DMi8 microscope, as well as cytokine analysis by qRT-PCR.

Inhibition of CD4$^+$ T cells

Mice were injected with the S1P receptor inhibitor FTY720 (fingolimod, Sigma-Aldrich, #SML0700-25MG) by intraperitoneal injection daily starting on model day 2 until the end of the 4-day model. In parallel, mice were administered CD4 neutralizing antibody (clone GK1.5, BioXCell, #BE0003) with 100 μg of anti-CD4 or rat IgG2b isotype control (clone LTF-2, BioXCell, #SKU: BE0090) via intraperitoneal injection on model days 2 and 4 separately. We assessed the inhibition of CD4$^+$ in the brain samples by flow cytometric analysis gating on CD45$^+$CD3$^+$ (FTY720) and CD3$^+$CD4$^+$ (anti-CD4).

Isolation of immune cells from mouse intestine and brain

To isolate the cellular infiltrate from the lamina propria in the gut of newborn mice, small intestine samples were cleared of mesentery, opened longitudinally, finely minced with scissors, and incubated in RPMI containing 2% fetal bovine serum (FBS) and 10 mM dithioerythritol (Sigma-Aldrich), which was prewarmed to 37°C. Tissue was incubated for 20 min with gentle agitation. Supernatants containing the enterocyte layer were then discarded. Lamina propria leukocytes were then isolated from the remaining tissue digestion (37°C, 40 min) in RPMI, containing 10% FBS, collagenase (100 U/ml) (Sigma-Aldrich), and deoxyribonuclease (15 μg/ml) (Sigma-Aldrich) with gentle agitation. Cells were then washed with RPMI (2% FBS) and filtered through a 70-μm strainer (Fisherbrand, 22-363-548) before being subjected to Percoll gradient separation (GE Healthcare, 17-0891-01). Isolated cells were then pelleted by centrifugation at 400*g* for 10 min, washed one time with ice-cold fluorescence-activated cell sorting (FACS) buffer [PBS with 0.05% bovine serum albumin (BSA)], and proceeded with flow cytometric studies or further purified for injection or organoid-based studies.

For isolation of immune cells from the brains of mice, animals were perfused via intracardiac injection with 10 ml of heparinized PBS (10 U/ml; Sigma-Aldrich, H3393-100KU) steadily and slowly until the liver was clear. The injection was introduced into the right atrium of the anesthetized animal with a 24-gauge needle (Butterfly infusion set, Abbott Laboratories, IL, USA, 50-3283-R1-12/89) through a small incision to the posterior end of the left ventricle. After perfusion to remove cells loosely attached to the endothelium, the animals were euthanized by decapitation, to allow for the entire brain to be isolated from the skull with minimal perturbation. Whole brains were then minced in cold PBS and filtered through 40-μm strainers (Falcon, 352340). Brain leukocytes were isolated using the Percoll gradient separation method and were pelleted by centrifugation

at 400*g* for 10 min, washed one time with ice-cold FACS buffer (PBS with 0.05% BSA), and proceeded with flow cytometric studies or further purified for injection or organoid-based studies.

Intracerebroventricular and intraperitoneal injections

For in vivo injection, single-cell suspensions of brain or intestine leukocytes were obtained as described above and further incubated with mouse CD4 (L3T4) Microbeads (Miltenyi Biotec, 130-117-043) according to the manufacturer's instructions. Cells were then washed and enriched by using the MACS cell separation system (LS Columns, 130-042-401; MidiMACS separator, 130-042-302; Miltenyi Biotec) before in vivo injection. For both intracerebroventricular and intraperitoneal injections, CD4 cells from brain or intestine were pooled from five mice with NEC or from mice without NEC, before resuspending in sterile PBS and injecting into *Rag1*$^{-/-}$ mice at P7. Brain tissues were harvested for qRT-PCR/immunohistochemistry assessment at P11. Successful reconstitution of cells was verified by imaging CD4-tomato-red signaling after 24 hours.

Brain and gut T cell receptor sequencing

To characterize the T cells harvested from the brains of mice with and without NEC, T cell receptor sequencing was performed. In brief, DNA was extracted from MACS-purified CD4$^+$ cells from control brain, control gut, diseased brain (NEC), and diseased gut (NEC) with QIAamp DNA Mini Kit (QIAGEN, 51304) according to the manufacturer's protocol. DNA samples were then subjected to immunoSEQ sequencing (Adaptive Biotechnologies) of the T cell receptor β-chain CDR3 regions, with primers annealing to V and J segments, resulting in amplification of rearranged V(D)J segments from each cell. Clonality and rearrangement sequences were obtained through immunoSEQ Analyzer software, and shared clones between brain and gut from each group (control brain versus control gut, NEC brain versus NEC gut) were plotted using pairwise scatter plot. Shared clone ratios (overlapping clones between brain and gut divided by all clones identified in the brain) were calculated for each data points in both control and diseased groups. To enrich the abundance of templates for meaningful sequencing analysis, DNA extracts from five animals were pooled into each sample and five data points were collected for analysis for each group.

Statistics

All data were analyzed using two-tailed Student's *t* test for comparison (GraphPad). Use of one-sided versus two-sided Student's *t* test is indicated in the figure legends; data from animal groups were normally distributed. Statistical significance was set at a *P* value of <0.05. All quantitative data are presented as means ± SD. All experiments were performed with at least three biological replicates and at least three animals per group.

SUPPLEMENTARY MATERIALS

stm.sciencemag.org/cgi/content/full/13/575/eaay6621/DC1

Materials and Methods

Fig. S1. Brain and intestinal histology in mice with experimental NEC resembles that in premature infants.

Fig. S2. Distribution of activated microglia and lymphocyte accumulation in NEC-associated brain injury in mice.

Fig. S3. NEC-associated brain injury is associated with microglial activation and correlates with intestinal injury in mice.

Fig. S4. Lymphocytes in NEC mouse brain are predominantly IFN-γ–producing CD4$^+$ T cells.

Fig. S5. Inhibition of lymphocyte migration does not reduce inflammation in the intestine of NEC mice.

Fig. S6. Ontogeny of neuronal gene expression in cultured mouse brain organoids.

Fig. S7. Neutralization of IFN-γ reverses the induction of NEC-associated brain injury in mice.

Table S1. Human brain specimen information.

Table S2. qRT-PCR gene and primer list.

Movie S1. Adoptively transferred NEC brain-derived CD4$^+$ T cells are localized in lateral ventricles and corpus callosum.

Movie S2. Control sham injection (PBS only) into lateral ventricles and corpus callosum reveals the absence of staining.

Data file S1. Individual-level data for all figures.

References (*51*–*54*)

View/request a protocol for this paper from *Bio-protocol*.

REFERENCES AND NOTES

1. J. Neu, W. A. Walker, Necrotizing enterocolitis. *N. Engl. J. Med.* **364**, 255–264 (2011).
2. B. J. Stoll, N. I. Hansen, E. F. Bell, M. C. Walsh, W. A. Carlo, S. Shankaran, A. R. Laptook, P. J. Sánchez, K. P. Van Meurs, M. Wyckoff, A. Das, E. C. Hale, M. Bethany Ball, N. S. Newman, K. Schibler, B. B. Poindexter, K. A. Kennedy, C. Michael Cotten, K. L. Watterberg, C. T. D'Angio, S. B. DeMauro, W. E. Truog, U. Devaskar, R. D. Higgins, Trends in care practices, morbidity, and mortality of extremely preterm Neonates, 1993-2012. *JAMA* **314**, 1039–1051 (2015).
3. C. P. Sodhi, M. D. Neal, R. Siggers, S. Sho, C. Ma, M. F. Branca, T. Prindle, A. M. Russo, A. Afrazi, M. Good, R. Browersinning, B. Firek, M. J. Morowitz, J. A. Ozolek, G. K. Gittes, T. R. Billiar, D. J. Hackam, Intestinal epithelial toll-like receptor 4 regulates goblet cell development and is required for necrotizing enterocolitis in mice. *Gastroenterology* **143**, 708–718.e5 (2012).
4. D. F. Nino, C. P. Sodhi, D. J. Hackam, Necrotizing enterocolitis: New insights into pathogenesis and mechanisms. *Nat. Rev. Gastroenterol. Hepatol.* **13**, 590–600 (2016).
5. K. Huang, S. Mukherjee, V. DesMarais, J. M. Albanese, E. Rafti, A. Draghi, L. A. Maher, K. M. Khanna, S. Mani, A. P. Matson, Targeting the PXR-TLR4 signaling pathway to reduce intestinal inflammation in an experimental model of necrotizing enterocolitis. *Pediatr. Res.* **83**, 1031–1040 (2018).
6. Y. Zhou, Y. Li, B. Zhou, K. Chen, Z. Lyv, D. Huang, B. Liu, Z. Xu, B. Xiang, S. Jin, X. Sun, Y. Li, Inflammation and apoptosis: Dual mediator role for toll-like receptor 4 in the development of necrotizing enterocolitis. *Inflamm. Bowel Dis.* **23**, 44–56 (2017).
7. T. Jilling, D. Simon, J. Lu, F. J. Meng, D. Li, R. Schy, R. B. Thomson, A. Soliman, M. Arditi, M. S. Caplan, The roles of bacteria and TLR4 in rat and murine models of necrotizing enterocolitis. *J. Immunol.* **177**, 3273–3282 (2006).
8. D. J. Hackam, C. P. Sodhi, Toll-like receptor-mediated intestinal inflammatory imbalance in the pathogenesis of necrotizing enterocolitis. *Cell. Mol. Gastroenterol. Hepatol.* **6**, 229–238.e1 (2018).
9. L. C. Duffy, M. A. Zielezny, V. Carrion, E. Griffiths, D. Dryja, M. Hilty, C. Rook, F. Morin III, Concordance of bacterial cultures with endotoxin and interleukin-6 in necrotizing enterocolitis. *Dig. Dis. Sci.* **42**, 359–365 (1997).
10. T. A. Shah, J. Meinzen-Derr, T. Gratton, J. Steichen, E. F. Donovan, K. Yolton, B. Alexander, V. Narendran, K. R. Schibler, Hospital and neurodevelopmental outcomes of extremely low-birth-weight infants with necrotizing enterocolitis and spontaneous intestinal perforation. *J. Perinatol.* **32**, 552–558 (2012).
11. S. R. Hintz, D. E. Kendrick, B. J. Stoll, B. R. Vohr, A. A. Fanaroff, E. F. Donovan, K. Poole, M. L. Blakely, L. Wright, R. Higgins, Neurodevelopmental and growth outcomes of extremely low birth weight infants after necrotizing enterocolitis. *Pediatrics* **115**, 696–703 (2005).
12. B. J. Stoll, N. I. Hansen, I. Adams-Chapman, A. A. Fanaroff, S. R. Hintz, B. Vohr, R. D. Higgins; National Institute of Child Health and Human Development Neonatal Research Network, Neurodevelopmental and growth impairment among extremely low-birth-weight infants with neonatal infection. *JAMA* **292**, 2357–2365 (2004).
13. D. F. Niño, Q. Zhou, Y. Yamaguchi, L. Y. Martin, S. Wang, W. B. Fulton, H. Jia, P. Lu, T. Prindle, F. Zhang, J. Crawford, Z. Hou, S. Mori, L. L. Chen, A. Guajardo, A. Fatemi, M. Pletnikov, R. M. Kannan, S. Kannan, C. P. Sodhi, D. J. Hackam, Cognitive impairments induced by necrotizing enterocolitis can be prevented by inhibiting microglial activation in mouse brain. *Sci. Transl. Med.* **10**, 471 (2018).
14. K. Suk, Lipocalin-2 as a therapeutic target for brain injury: An astrocentric perspective. *Prog. Neurobiol.* **144**, 158–172 (2016).
15. C. U. A. Kloss, M. Bohatschek, G. W. Kreutzberg, G. Raivich, Effect of lipopolysaccharide on the morphology and integrin immunoreactivity of ramified microglia in the mouse brain and in cell culture. *Exp. Neurol.* **168**, 32–46 (2001).
16. Y. Wolf, S. Yona, K. W. Kim, S. Jung, Microglia, seen from the CX3CR1 angle. *Front. Cell. Neurosci.* **7**, 26 (2013).
17. K. Devraj, S. Guérit, J. Macas, Y. Reiss, An in vivo blood-brain barrier permeability assay in mice using fluorescently labeled tracers. *J. Vis. Exp.* **132**, 57038 (2018).
18. T. Hla, V. Brinkmann, Sphingosine 1-phosphate (S1P): Physiology and the effects of S1P receptor modulation. *Neurology* **76**, S3–S8 (2011).

19. J. Naessens, J. P. Scheerlinck, E. V. De Buysscher, D. Kennedy, M. Sileghem, Effective in vivo depletion of T cell subpopulations and loss of memory cells in cattle using mouse monoclonal antibodies. *Vet. Immunol. Immunopathol.* **64**, 219–234 (1998).
20. E. A. Susaki, K. Tainaka, D. Perrin, F. Kishino, T. Tawara, T. M. Watanabe, C. Yokoyama, H. Onoe, M. Eguchi, S. Yamaguchi, T. Abe, H. Kiyonari, Y. Shimizu, A. Miyawaki, H. Yokota, H. R. Ueda, Whole-brain imaging with single-cell resolution using chemical cocktails and computational analysis. *Cell* **157**, 726–739 (2014).
21. C. E. Egan, C. P. Sodhi, M. Good, J. Lin, H. Jia, Y. Yamaguchi, P. Lu, C. Ma, M. F. Branca, S. Weyandt, W. B. Fulton, D. F. Nino, T. Prindle Jr., J. A. Ozolek, D. J. Hackam, Toll-like receptor 4-mediated lymphocyte influx induces neonatal necrotizing enterocolitis. *J. Clin. Invest.* **126**, 495–508 (2016).
22. T. Korn, A. Kallies, T cell responses in the central nervous system. *Nat. Rev. Immunol.* **17**, 179–194 (2017).
23. C. A. Dendrou, L. Fugger, M. A. Friese, Immunopathology of multiple sclerosis. *Nat. Rev. Immunol.* **15**, 545–558 (2015).
24. L. Gu, Z. Jian, C. Stary, X. Xiong, T cells and cerebral ischemic stroke. *Neurochem. Res.* **40**, 1786–1791 (2015).
25. D. Zierath, J. Schulze, A. Kunze, O. Drogomiretskiy, D. Nhan, B. Jaspers, A. Dressel, K. Becker, The immunologic profile of adoptively transferred lymphocytes influences stroke outcome of recipients. *J. Neuroimmunol.* **263**, 28–34 (2013).
26. A. Villegas-Mendez, R. Greig, T. N. Shaw, J. B. de Souza, E. Gwyer Findlay, J. S. Stumhofer, J. C. Hafalla, D. G. Blount, C. A. Hunter, E. M. Riley, K. N. Couper, IFN-γ–producing CD4+ T cells promote experimental cerebral malaria by modulating CD8+T cell accumulation within the brain. *J. Immunol.* **189**, 968–979 (2012).
27. D. Yang, Y. Y. Sun, S. K. Bhaumik, Y. Li, J. M. Baumann, X. Lin, Y. Zhang, S. H. Lin, R. S. Dunn, C. Y. Liu, F. S. Shie, Y. H. Lee, M. Wills-Karp, C. A. Chougnet, S. G. Kallapur, I. P. Lewkowich, D. M. Lindquist, K. Murali-Krishna, C. Y. Kuan, Blocking lymphocyte trafficking with FTY720 prevents inflammation-sensitized hypoxic-ischemic brain injury in newborns. *J. Neurosci.* **34**, 16467–16481 (2014).
28. A. Nazmi, A. M. Albertsson, E. Rocha-Ferreira, X. Zhang, R. Vontell, A. Zelco, M. Rutherford, C. Zhu, G. Nilsson, C. Mallard, H. Hagberg, J. C. Y. Lai, J. W. Leavenworth, X. Wang, Lymphocytes contribute to the pathophysiology of neonatal brain injury. *Front. Neurol.* **9**, 159 (2018).
29. N. Fathali, R. P. Ostrowski, Y. Hasegawa, T. Lekic, J. Tang, J. H. Zhang, Splenic immune cells in experimental neonatal hypoxia-ischemia. *Transl. Stroke Res.* **4**, 208–219 (2013).
30. Á. C. Murphy, S. J. Lalor, M. A. Lynch, K. H. G. Mills, Infiltration of Th1 and Th17 cells and activation of microglia in the CNS during the course of experimental autoimmune encephalomyelitis. *Brain Behav. Immun.* **24**, 641–651 (2010).
31. K. Hirota, J. H. Duarte, M. Veldhoen, E. Hornsby, Y. Li, D. J. Cua, H. Ahlfors, C. Wilhelm, M. Tolaini, U. Menzel, A. Garefalaki, A. J. Potocnik, B. Stockinger, Fate mapping of IL-17-producing T cells in inflammatory responses. *Nat. Immunol.* **12**, 255–263 (2011).
32. I. E. Papageorgiou, A. Lewen, L. V. Galow, T. Cesetti, J. Scheffel, T. Regen, U. K. Hanisch, O. Kann, TLR4-activated microglia require IFN-γ to induce severe neuronal dysfunction and death in situ. *Proc. Natl. Acad. Sci. U.S.A.* **113**, 212–217 (2016).
33. I. M. Stromnes, J. M. Goverman, Active induction of experimental allergic encephalomyelitis. *Nat. Protoc.* **1**, 1810–1819 (2006).
34. K. Berer, M. Mues, M. Koutrolos, Z. AlRasbi, M. Boziki, C. Johner, H. Wekerle, G. Krishnamoorthy, Commensal microbiota and myelin autoantigen cooperate to trigger autoimmune demyelination. *Nature* **479**, 538–541 (2011).
35. T. Gaber, C. Strehl, F. Buttgereit, Metabolic regulation of inflammation. *Nat. Rev. Rheumatol.* **13**, 267–279 (2017).
36. B. Winkler, J. Aulenbach, T. Meyer, A. Wiegering, M. Eyrich, P. G. Schlegel, V. Wiegering, Formula-feeding is associated with shift towards Th1 cytokines. *Eur. J. Nutr.* **54**, 129–138 (2015).
37. A. Wang, H. H. Luan, R. Medzhitov, An evolutionary perspective on immunometabolism. *Science* **363**, 6423 (2019).
38. C. Benakis, D. Brea, S. Caballero, G. Faraco, J. Moore, M. Murphy, G. Sita, G. Racchumi, L. Ling, E. G. Pamer, C. Iadecola, J. Anrather, Commensal microbiota affects ischemic stroke outcome by regulating intestinal γδ T cells. *Nat. Med.* **22**, 516–523 (2016).
39. Y. Feng, X. He, S. Luo, X. Chen, S. Long, F. Liang, T. Shi, Z. Pei, Z. Li, Chronic colitis induces meninges traffic of gut-derived T cells, unbalances M1 and M2 microglia/macrophage and increases ischemic brain injury in mice. *Brain Res.* **1707**, 8–17 (2019).
40. B. C. MacQueen, R. D. Christensen, C. C. Yost, D. K. Lambert, V. L. Baer, M. J. Sheffield, P. V. Gordon, M. J. Cody, E. Gerday, R. Schlaberg, J. Lowe, J. G. Shepherd, Elevated fecal calprotectin levels during necrotizing enterocolitis are associated with activated neutrophils extruding neutrophil extracellular traps. *J. Perinatol.* **36**, 862–869 (2016).
41. K. MohanKumar, K. Namachivayam, K. C. Chapalamadugu, S. A. Garzon, M. H. Premkumar, S. M. Tipparaju, A. Maheshwari, Smad7 interrupts TGF-β signaling in intestinal macrophages and promotes inflammatory activation of these cells during necrotizing enterocolitis. *Pediatr. Res.* **79**, 951–961 (2016).
42. J. H. Weitkamp, T. Koyama, M. T. Rock, H. Correa, J. A. Goettel, P. Matta, K. Oswald-Richter, M. J. Rosen, B. G. Engelhardt, D. J. Moore, D. B. Polk, Necrotising enterocolitis is characterised by disrupted immune regulation and diminished mucosal regulatory (FOXP3)/effector (CD4, CD8) T cell ratios. *Gut* **62**, 73–82 (2013).
43. P. Lu, C. P. Sodhi, H. Jia, S. Shaffiey, M. Good, M. F. Branca, D. J. Hackam, Animal models of gastrointestinal and liver diseases. Animal models of necrotizing enterocolitis: Pathophysiology, translational relevance, and challenges. *Am. J. Physiol. Gastrointest. Liver Physiol.* **306**, G917–G928 (2014).
44. G. Biouss, L. Antounians, B. Li, J. S. O'Connell, S. Seo, V. D. Catania, J. Guadagno, A. Rahman, E. Zani-Ruttenstock, N. Svergun, A. Pierro, A. Zani, Experimental necrotizing enterocolitis induces neuroinflammation in the neonatal brain. *J. Neuroinflammation* **16**, 97 (2019).
45. A. Brunse, A. Abbaspour, P. T. Sangild, Brain barrier disruption and region-specific neuronal degeneration during necrotizing enterocolitis in preterm pigs. *Dev. Neurosci.* **40**, 198–208 (2018).
46. J. Sun, X. Pan, L. I. Christiansen, X.-L. Yuan, K. Skovgaard, D. E. W. Chatterton, S. S. Kaalund, F. Gao, P. T. Sangild, S. Pankratova, Necrotizing enterocolitis is associated with acute brain responses in preterm pigs. *J. Neuroinflammation* **15**, 180 (2018).
47. J. Lu, E. C. Claud, Connection between gut microbiome and brain development in preterm infants. *Dev. Psychobiol.* **61**, 739–751 (2019).
48. D. J. Hackam, C. P. Sodhi, M. Good, New insights into necrotizing enterocolitis: From laboratory observation to personalized prevention and treatment. *J. Pediatr. Surg.* **54**, 398–404 (2019).
49. Z. Su, H. Lu, H. Jiang, H. Zhu, Z. Li, P. Zhang, P. Ni, H. Shen, W. Xu, H. Xu, IFN-γ-producing Th17 cells bias by HMGB1-T-bet/RUNX3 axis might contribute to progression of coronary artery atherosclerosis. *Atherosclerosis* **243**, 421–428 (2015).
50. L. Duan, C.-Y. Wang, J. Chen, Q. Gong, P. Zhu, F. Zheng, Z. Tan, F. Gong, M. Fang, High-mobility group box 1 promotes early acute allograft rejection by enhancing IL-6-dependent Th17 alloreactive response. *Lab. Invest.* **91**, 43–53 (2011).
51. Z. Wen, H. N. Nguyen, Z. Guo, M. A. Lalli, X. Wang, Y. Su, N. S. Kim, K. J. Yoon, J. Shin, C. Zhang, G. Makri, D. Nauen, H. Yu, E. Guzman, C. H. Chiang, N. Yoritomo, K. Kaibuchi, J. Zou, K. M. Christian, L. Cheng, C. A. Ross, R. L. Margolis, G. Chen, K. S. Kosik, H. Song, G. L. Ming, Synaptic dysregulation in a human iPS cell model of mental disorders. *Nature* **515**, 414–418 (2014).
52. D. Pamies, A. Bal-Price, C. Chesné, S. Coecke, A. Dinnyes, C. Eskes, R. Grillari, G. Gstraunthaler, T. Hartung, P. Jennings, M. Leist, U. Martin, R. Passier, J. C. Schwamborn, G. N. Stacey, H. Ellinger-Ziegelbauer, M. Daneshian, Advanced good cell culture practice for human primary, stem cell-derived and organoid models as well as microphysiological systems. *ALTEX* **35**, 353–378 (2018).
53. B. E. Kerman, H. J. Kim, K. Padmanabhan, A. Mei, S. Georges, M. S. Joens, J. A. J. Fitzpatrick, R. Jappelli, K. J. Chandross, P. August, F. H. Gage, In vitro myelin formation using embryonic stem cells. *Development* **142**, 2213–2225 (2015).
54. C. McQuin, A. Goodman, V. Chernyshev, L. Kamentsky, B. A. Cimini, K. W. Karhohs, M. Doan, L. Ding, S. M. Rafelski, D. Thirstrup, W. Wiegraebe, S. Singh, T. Becker, J. C. Caicedo, A. E. Carpenter, CellProfiler 3.0: Next-generation image processing for biology. *PLOS Biol.* **16**, e2005970 (2018).

Funding: D.J.H. was funded by grants RO1DK117186, RO1DK121824, and RO1GM078238 from the NIH. H.J. was funded by grants RO1AI148446 and R21AI49321. **Author contributions:** Q.Z. and C.P.S. designed, planned, and conducted the experiments; developed the transgenic mice; analyzed results; assembled the figures; and wrote and edited the manuscript. D.J.H. conceived the study, planned the experiments, reviewed the results, and wrote and edited the manuscript. Y.Y., P.L., D.P., T.P., S.W., L.L.C., W.B.F., H.J., D.F.N., and M.M. conducted NEC mouse model experiments, immunohistochemistry, and confocal microscopy. L.L.C. obtained human pathology specimens and reviewed results. **Competing interests:** D.J.H. and C.P.S. are coinventors on patent US9562066B2 entitled "Oral therapy of necrotizing enterocolitis" and US20130281395A1 entitled "Novel TLR4 inhibitors for the treatment of human infectious and inflammatory disorders." D.J.H., C.P.S., and D.P. are coinventors on patent US201562248063P entitled "Dendrimer compositions and use in treatment of necrotizing enterocolitis and other gastrointestinal disorders." D.P. is coinventor on patent US16/077,411 entitled "Compositions and methods for neuralgenesis," which is licensed to AxoSim. The other authors declare no competing interests. **Data and materials availability:** All data associated with this study are present in the paper or the Supplementary Materials.

Submitted 8 July 2019
Resubmitted 27 April 2020
Accepted 18 August 2020
Published 6 January 2021
10.1126/scitranslmed.aay6621

Citation: Q. Zhou, D. F. Niño, Y. Yamaguchi, S. Wang, W. B. Fulton, H. Jia, P. Lu, T. Prindle Jr., D. Pamies, M. Morris, L. L. Chen, C. P. Sodhi, D. J. Hackam, Necrotizing enterocolitis induces T lymphocyte–mediated injury in the developing mammalian brain. *Sci. Transl. Med.* **13**, eaay6621 (2021).

Science Translational Medicine

Necrotizing enterocolitis induces T lymphocyte–mediated injury in the developing mammalian brain

Qinjie Zhou, Diego F. Niño, Yukihiro Yamaguchi, Sanxia Wang, William B. Fulton, Hongpeng Jia, Peng Lu, Thomas Prindle, Jr., David Pamies, Meaghan Morris, Liam L. Chen, Chhinder P. Sodhi and David J. Hackam

Sci Transl Med **13**, eaay6621.
DOI: 10.1126/scitranslmed.aay6621

Elucidating the gut-brain connection in necrotizing enterocolitis

Necrotizing enterocolitis (NEC) is a devastating disease of premature infants characterized by acute intestinal necrosis and long-term neurological dysfunction, through mechanisms that are poorly understood. In new work, Zhou *et al*. study a neonatal mouse model of NEC, human brain autopsy specimens from infants with and without NEC, and human and mouse brain organoids. They report that $CD4^+$ T lymphocytes, partially of intestinal origin, damage the developing brain of neonatal mice in the setting of NEC through the release of IFN-γ. These findings suggest that early management of intestinal injury, or control of the lymphocyte response, could improve neurological impairment in children with NEC.

Science Translational Medicine (ISSN 1946-6242) is published by the American Association for the Advancement of Science, 1200 New York Avenue NW, Washington, DC 20005. The title *Science Translational Medicine* is a registered trademark of AAAS.